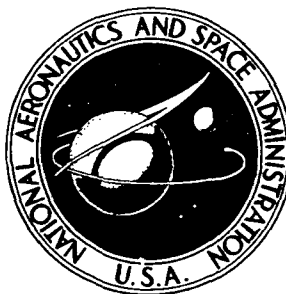


**NASA TECHNICAL  
MEMORANDUM**



**NASA TM X-3433**

**NASA TM X-3433**

**PRELIMINARY STUDY OF EFFECTS  
OF WINGLETS ON WING FLUTTER**

*Robert V. Doggett, Jr., and Moses G. Farmer*

*Langley Research Center*

*Hampton, Va. 23665*



**NATIONAL AERONAUTICS AND SPACE ADMINISTRATION • WASHINGTON, D. C. • DECEMBER 1976**

1. Report No. NASA TM X-3433		2. Government Accession No.		3. Recipient's Catalog No.	
4. Title and Subtitle <b>PRELIMINARY STUDY OF EFFECTS OF WINGLETS ON WING FLUTTER</b>				5. Report Date December 1976	
				6. Performing Organization Code	
7. Author(s) Robert V. Doggett, Jr., and Moses G. Farmer				8. Performing Organization Report No. L-10963	
9. Performing Organization Name and Address NASA Langley Research Center Hampton, VA 23665				10. Work Unit No. 505-02-21-01	
				11. Contract or Grant No.	
12. Sponsoring Agency Name and Address National Aeronautics and Space Administration Washington, DC 20546				13. Type of Report and Period Covered Technical Memorandum	
				14. Sponsoring Agency Code	
15. Supplementary Notes					
16. Abstract  Some experimental flutter results are presented over a Mach number range from about 0.70 to 0.95 for a simple, swept, tapered, flat-plate wing model having a planform representative of subsonic transport airplanes and for the same wing model equipped with two different upper surface winglets. Both winglets had the same planform and area (about 2 percent of the basic-wing area); however, one weighed about 0.3 percent of the basic-wing weight, and the other weighed about 1.8 percent of the wing weight. The addition of the lighter winglet reduced the wing-flutter dynamic pressure by about 3 percent; the heavier winglet reduced the wing-flutter dynamic pressure by about 12 percent. The experimental flutter results are compared at a Mach number of 0.80 with analytical flutter results obtained by using doublet-lattice and lifting-surface (kernel-function) unsteady aerodynamic theories.					
17. Key Words (Suggested by Author(s)) Flutter Winglets Nonplanar surfaces			18. Distribution Statement  Unclassified - Unlimited  Subject Category 32		
19. Security Classif. (of this report) Unclassified		20. Security Classif. (of this page) Unclassified		21. No. of Pages 23	22. Price* \$3.25

# PRELIMINARY STUDY OF EFFECTS OF WINGLETS ON WING FLUTTER

Robert V. Doggett, Jr., and Moses G. Farmer  
Langley Research Center

## SUMMARY

Some experimental flutter results are presented over a Mach number range from about 0.70 to 0.95 for a simple, swept, tapered, flat-plate wing model having a planform representative of subsonic transport airplanes and for the same wing model equipped with two different upper surface winglets. Both winglets had the same planform and area (about 2 percent of the basic-wing area); however, one weighed about 0.3 percent of the basic-wing weight, and the other weighed about 1.8 percent of the wing weight. The addition of the lighter winglet reduced the wing-flutter dynamic pressure by about 3 percent; the heavier winglet reduced the wing-flutter dynamic pressure by about 12 percent. The experimental flutter results are compared at a Mach number of 0.80 with analytical flutter results obtained by using doublet-lattice and lifting-surface (kernel-function) unsteady aerodynamic theories.

## INTRODUCTION

Currently there is considerable interest in reducing airplane fuel consumption. One way to reduce airplane fuel usage is through improved aerodynamic efficiency. Some recent work at the Langley Research Center has indicated that significant reductions in drag due to lift can be achieved by the addition of small, nearly vertical, wing-like surfaces called winglets at the tip of the main wing. An approach to winglet design is presented in reference 1 which also includes results from winglet applications to a representative first-generation subsonic transport wing. Some results from winglet applications to a representative second-generation transport wing are presented in reference 2. An attractive feature of the winglet is that it not only can be incorporated in new airplane designs but it also has the potential for use as a modification to current designs. However, the addition of winglets to current designs does raise the question of what are the structural and dynamic implications. A specific question that must be addressed is the possible winglet effects on flutter. Consequently, some wind-tunnel flutter-model studies were made in the Langley transonic dynamics tunnel by using a relatively simple cantilever, flat-plate wing model that was tested with and without an upper surface winglet. The purpose of

this paper is to present the results from this study. It should be pointed out that some winglet aerodynamic studies have considered having both upper surface and lower surface winglets – a large one mounted rearward on the upper surface at the wing tip and a smaller one mounted forward on the lower surface at the tip. (See ref. 1.) Lower surface winglets were not included in the present study. The basic-wing model used here had a planform representative of current subsonic transport designs. The same wing model was tested with and without two different winglets mounted on the upper surface at the wing tip. The winglets were, like the wing, flat-plate models and weighed about 0.3 percent and 1.8 percent of the basic wing weight, respectively. Both winglets had the same planform and area, about 2 percent of the main wing area. Experimental flutter results are presented over the Mach number range from about 0.70 to 0.95. Some experimental results are compared with analytical results obtained by using doublet-lattice and lifting-surface (kernel-function) unsteady aerodynamic theories.

## SYMBOLS

Measurements and calculations were made in U.S. Customary Units and are presented in both the International System of Units (SI) and U.S. Customary Units.

$b_r$	reference semichord
$f$	frequency
$f_f$	flutter frequency
$f_r$	reference frequency, measured frequency of third natural mode
$f_1$	measured frequency of first natural mode
$f_2$	measured frequency of second natural mode
$m$	mass
$q$	dynamic pressure, $\frac{1}{2} \rho V^2$
$V$	velocity
$V_I$	flutter-speed index parameter, $V / (b_r \omega_r \bar{\mu})$

v	reference volume
$\mu$	mass-ratio parameter, $\frac{m}{\rho v}$
$\rho$	density
$\omega_r$	reference circular frequency, $2\pi f_r$

Subscripts:

c	calculated
e	experimental

## MODELS

### Description

The basic-wing configuration used in this investigation was a cantilever-mounted semispan wing that had a planform representative of current subsonic transport wings. The full-span aspect ratio was 6.37 with no dihedral, the leading-edge sweep was  $38.2^\circ$ , and the taper ratio was 0.20. Two other models, consisting of the basic configuration with a winglet mounted on the upper surface at the wing tip, were tested in an effort to determine the winglet effects on the wing-flutter characteristics. A photograph of one of the models mounted in the wind tunnel is presented in figure 1. Sketches giving the geometric properties of the wing and winglet are presented in figure 2. It should be pointed out that since the winglets used here were uncambered nonlifting surfaces, only the planform aerodynamic effects and structural mass and stiffness effects of the winglets were evaluated. Both winglets had the same planform and area, about 2 percent of the wing area. The primary difference between the two winglets was in structural mass and stiffness. The winglets weighed about 0.3 percent and 1.8 percent of the basic-wing weight, respectively. The two winglet configurations will be referred to hereinafter as the light-winglet model and the heavy-winglet model, respectively. The winglet was mounted aft on the wing-tip chord and was canted outward  $17\frac{1}{2}^\circ$  from a plane perpendicular to the plane of the wing. The winglet had a leading-edge sweep of  $39.9^\circ$ , a taper ratio of 0.33, and a full-span aspect ratio of 5.00.

The models were constructed of constant-thickness aluminum-alloy plate. The plate thicknesses were 0.483 cm (0.190 in.) for the wing, 0.081 cm (0.032 in.) for the light winglet, and 0.483 cm (0.190 in.) for the heavy winglet. The leading edges of the plate

models were rounded, and the trailing edges of the wing and heavy winglet were beveled. The flat plate was extended inboard of the model root to provide a base for clamping the models in a cantilever fashion along the forward 80 percent of the root chord. The models were clamped only partially along the root chord in order to provide an approximate simulation of an actual airplane wing-root condition.

The wing was instrumented with electric resistance-type strain gages to measure dynamic response.

### Physical Properties and Vibration Characteristics

The total measured mass properties of the three models are presented in table I. The first four natural frequencies were measured for the basic-wing and heavy-winglet models. The first three frequencies were measured for the light-winglet model. The measured values are given in table II along with the first five calculated natural frequencies of the basic-wing and heavy-winglet models and the first seven calculated frequencies of the light-winglet model. The corresponding calculated natural-mode nodal patterns are presented in figure 3. Note that the winglet has been rotated into the wing plane for clarity. Also included in figure 3 are the measured node lines for the first four basic-wing-model modes and the first three heavy-winglet-model modes. The calculated and measured nodal patterns are very similar. The measured node lines were obtained by the 1g sand technique. The calculated modal data were obtained by using the NASTRAN<sup>®</sup> (NASA Structural Analysis) Computer Program (refs. 3 and 4). Quadri-lateral structural finite elements (NASTRAN QUAD2) were used to model the structure. Ninety elements were used for the wing portion of all three models; 27 elements were used for the winglets. The arrangement of the elements is shown in figure 4.

## FLUTTER EXPERIMENTS

### Wind Tunnel

The experiment was conducted in the Langley transonic dynamics tunnel. The tunnel has a 4.88-m (16-ft) square test section with cropped corners. The tunnel is a slotted-throat, single-return wind tunnel equipped to use either air or Freon-12 as the test medium at stagnation pressures from near vacuum to about atmospheric at Mach numbers up to 1.2. Only Freon-12 was used for the present investigation. The tunnel is of the continuous-operation type and is powered by a motor-driven fan. Both test-section Mach number and density are continuously controllable. The tunnel is equipped with four quick-opening bypass valves which can be operated to reduce test-section dynamic pressure and Mach number rapidly when flutter occurs.

## Test Procedure

The same general procedure was used for all the tests. The determination of a typical flutter point proceeded as follows: With the tunnel evacuated to a low stagnation pressure, the fan speed was increased until the desired test-section Mach number was reached. The test-section Mach number was then held nearly constant, and the test-section density was gradually increased by adding Freon-12 to the tunnel through an expansion valve until flutter was reached. The test-section dynamic pressure and Mach number were then rapidly decreased by opening the four bypass valves. The actuation of the bypass valves also locked the tunnel instruments so that the tunnel conditions necessary to describe the flutter point completely could be recorded after precautions had been taken to save the model. The compressor speed was then decreased to a point well below the flutter condition, and the bypass valves were closed. This process was repeated several times to define the flutter boundary over the Mach number range of interest.

During each flutter condition the outputs from the bending and torsion resistance-wire strain gages mounted near the model root were recorded on an oscillograph. From these oscillograph records the flutter frequencies were determined. The first three natural frequencies for each model were checked before and after each tunnel test to determine whether the model had been damaged.

## FLUTTER ANALYSIS

Flutter calculations were made for all three models at a Mach number of 0.80. The flutter equations in matrix notation were expressed in terms of generalized modal coordinates, and the traditional V-G method of solution, automated essentially as described in reference 5, was used. The calculated natural frequencies and mode shapes were used in the analysis. The first five modes were used for the basic-wing and the heavy-winglet models; the first seven modes were used for the light-winglet model. The reader should note that the choice of seven modes for the light-winglet-model analysis against five modes for the other two models was somewhat arbitrary. It is believed that had only five modes been used for the light-winglet-model analysis, the flutter results would have been essentially the same as those obtained by using seven modes. Surface spline functions (ref. 6) were used to interpolate the calculated modal deflections to the modal displacements and to the streamwise slopes required to determine the unsteady aerodynamic forces. Calculations were made by using both doublet-lattice unsteady aerodynamic theory (refs. 7 and 8) and subsonic lifting-surface (kernel-function) theory (ref. 9). The doublet-lattice paneling arrangement consisted of 186 boxes on the wing and 72 boxes on the winglet arranged as shown in figure 5. The locations of the 36 kernel-function collocation points used are indicated by the solid-circle symbols in figure 5. In the

kernel-function calculations no aerodynamic effects of the winglet were included. Doublet-lattice calculations were made both with and without the inclusion of winglet unsteady aerodynamic effects.

## RESULTS AND DISCUSSION

The basic experimental flutter results are presented in figure 6 as the variations with Mach number of the mass-ratio parameter  $\mu$ , of the flutter-frequency ratio  $f_f/f_r$ , and of the flutter-speed index parameter  $V_I$ . The mass-ratio parameter  $\mu$  is defined as the ratio of the total model mass to the mass of a representative surrounding volume of test medium. The volume used here is that contained in the conical frustums generated by revolving each wing chord (and winglet chord) about its midpoint. These volumes were  $69\,260\text{ cm}^3$  ( $4226.4\text{ in}^3$ ) for the basic-wing model and  $69\,460\text{ cm}^3$  ( $4238.8\text{ in}^3$ ) for both winglet configurations. The third measured natural frequency was used as the reference frequency  $f_r$ . The semichord at the basic-wing three-quarter-span station, which was used as the reference length  $b_r$ , was 9.36 cm (3.685 in.). The flutter-speed-index-parameter curves represent stability boundaries with the stable region below the curve. This parameter depends on the physical properties of the model, in particular the stiffness, and is proportional to the square root of the dynamic pressure.

No unusual trends are shown by the data presented in figure 6 for all three configurations studied. The flutter boundaries are similar to those usually observed: namely, a gradual decrease in flutter speed occurs as the subsonic Mach number is increased. Flutter data were not obtained at sufficiently high Mach numbers to define the minimum flutter speed which usually occurs in the transonic regime.

A comparison of the flutter boundaries for all three models may be made by examining the data presented in figure 7 where the variations of flutter-speed index parameter and flutter dynamic pressure with Mach number are shown. Note that the addition of the winglet to the basic wing did have an adverse effect on the flutter characteristics, that is, the heavier the winglet the greater the effect. In general, the addition of the light and heavy winglets resulted in flutter dynamic-pressure reductions over the Mach number range studied of about 3 percent and 12 percent, respectively.

Flutter analyses were made at a Mach number  $M$  of 0.80 for all three model configurations by using kernel-function and doublet-lattice unsteady aerodynamic theories. The density values used in the calculations were obtained by interpolating the mass-ratio curves in figure 6. The analytical results are presented in figure 8 as the variation of the ratio of flutter frequency to reference frequency  $f_f/f_r$  and of dynamic pressure  $q$  with winglet weight relative to wing weight. The experimental results (plotted from the curves in figs. 6 and 7 for  $M = 0.80$ ) for this Mach number are also included in figure 8. The



kernel-function results presented include only wing unsteady aerodynamic forces. That is, only the structural effects of the winglet were included in the analysis. Doublet-lattice results are presented both with and without the inclusion of winglet unsteady aerodynamic forces. It can be seen that all of the analytical results are in good agreement with their corresponding experimental results (less than 10-percent variation in flutter frequency and less than 5-percent variation in dynamic pressure).

#### CONCLUDING REMARKS

The effects of the addition of two different upper surface winglets at the tip of a basic wing have been determined experimentally over the Mach number range from about 0.70 to 0.95 in the Langley transonic dynamics tunnel. The cantilever-mounted flat-plate wing had a planform representative of subsonic transport airplanes. The two flat-plate winglets had the same area and planform but differed from one another in mass and stiffness. One weighed about 0.3 percent and the other weighed about 1.8 percent of the basic-wing weight. The addition of the lighter winglet reduced the wing-flutter dynamic pressure by about 3 percent; the addition of the heavier winglet produced about a 12-percent reduction. The experimental results were compared at a Mach number of 0.80 with calculated results obtained by using kernel-function and doublet-lattice unsteady aerodynamic theories. The individual calculated results were in good agreement with corresponding experimental results for all three model configurations.

Langley Research Center  
National Aeronautics and Space Administration  
Hampton, VA 23665  
September 29, 1976

## REFERENCES

1. Whitcomb, Richard T.: A Design Approach and Selected Wind-Tunnel Results at High Subsonic Speeds for Wing-Tip Mounted Winglets. NASA TN D-8260, 1976.
2. Flechner, Stuart G.; Jacobs, Peter F.; and Whitcomb, Richard T.: A High Subsonic Speed Wind-Tunnel Investigation of Winglets on a Representative Second-Generation Jet Transport Wing. NASA TN D-8264, 1976.
3. MacNeal, Richard H., ed.: The NASTRAN Theoretical Manual. NASA SP-221, 1970.
4. McCormick, Caleb W., ed.: The NASTRAN User's Manual. NASA SP-222, 1970.
5. Desmarais, Robert N.; and Bennett, Robert M.: An Automated Procedure for Computing Flutter Eigenvalues. J. Aircraft, vol. 11, no. 2, Feb. 1974, pp. 75-80.
6. Harder, Robert L.; and Desmarais, Robert N.: Interpolation Using Surface Splines. J. Aircraft, vol. 9, no. 2, Feb. 1972, pp. 189-191.
7. Giesing, J. P.; Kalman, T. P.; and Rodden, W. P.: Subsonic Unsteady Aerodynamics for General Configurations. Part I, Vol. I - Direct Application of the Nonplanar Doublet-Lattice Method. AFFDL-TR-71-5, Pt. I, Vol. I, U.S. Air Force, Nov. 1971. (Available from DDC as AD 891 403L.)
8. Giesing, J. P.; Kalman, T. P.; and Rodden, W. P.: Subsonic Unsteady Aerodynamics for General Configurations. Part I, Vol. II - Computer Program H7WC. AFFDL-TR-71-5, Pt. I, Vol. II, U.S. Air Force, Nov. 1971. (Available from DDC as AD 892 535L.)
9. Watkins, Charles E.; Woolston, Donald S.; and Cunningham, Herbert J.: A Systematic Kernel Function Procedure for Determining Aerodynamic Forces on Oscillating or Steady Finite Wings at Subsonic Speeds. NASA TR R-48, 1959.

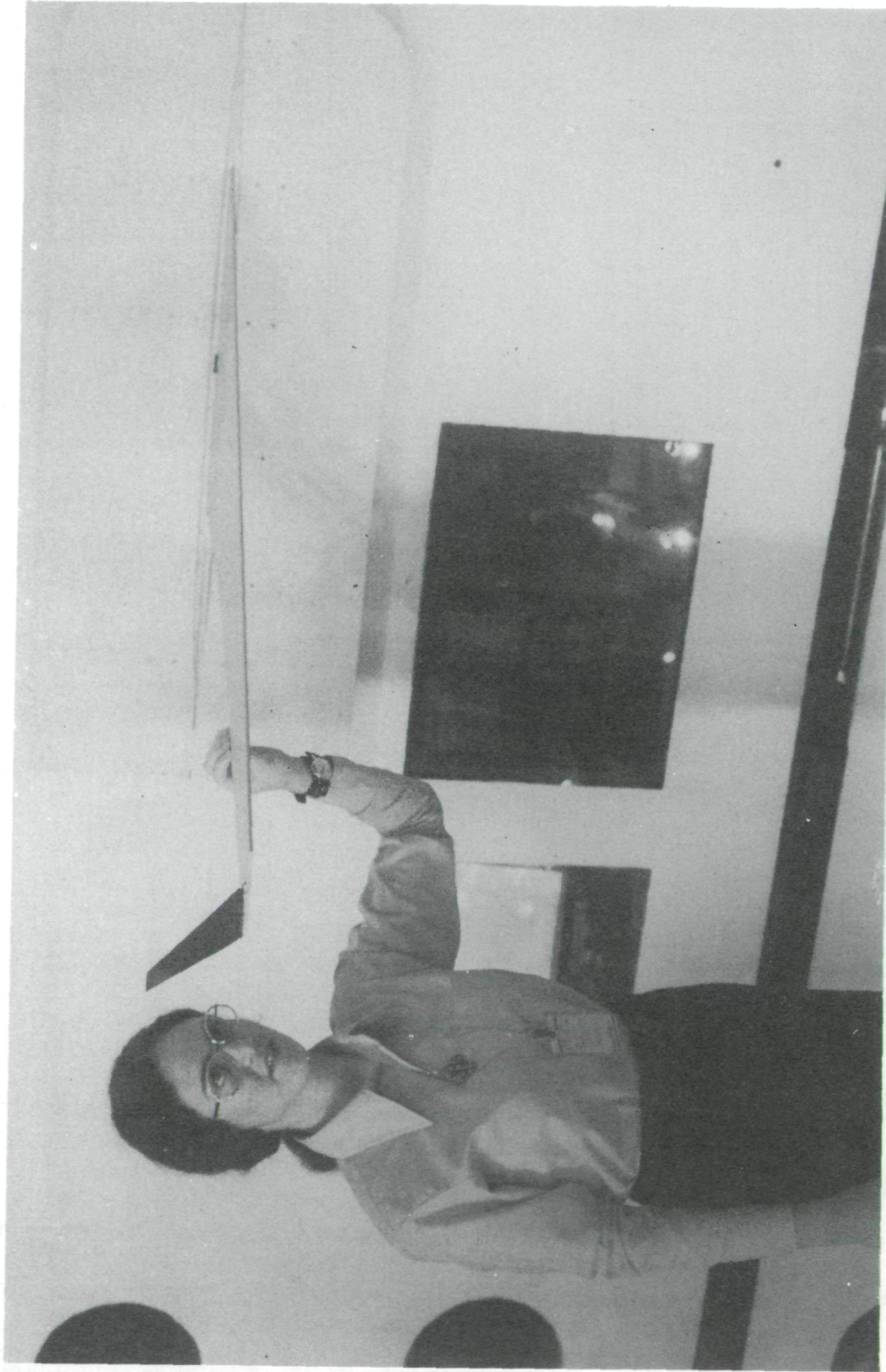
TABLE I.- MODEL MASS PROPERTIES

Model	Wing portion		Winglet portion		Total	
	kg	slugs	kg	slugs	kg	slugs
Basic wing . . . . .	3.550	0.2433	-----	-----	3.550	0.2433
Light winglet . . . . .	3.550	0.2433	0.0113	0.0008	3.5613	0.2441
Heavy winglet . . . . .	3.550	0.2433	0.0630	0.0043	3.6130	0.2476

TABLE II.- MODEL NATURAL FREQUENCIES

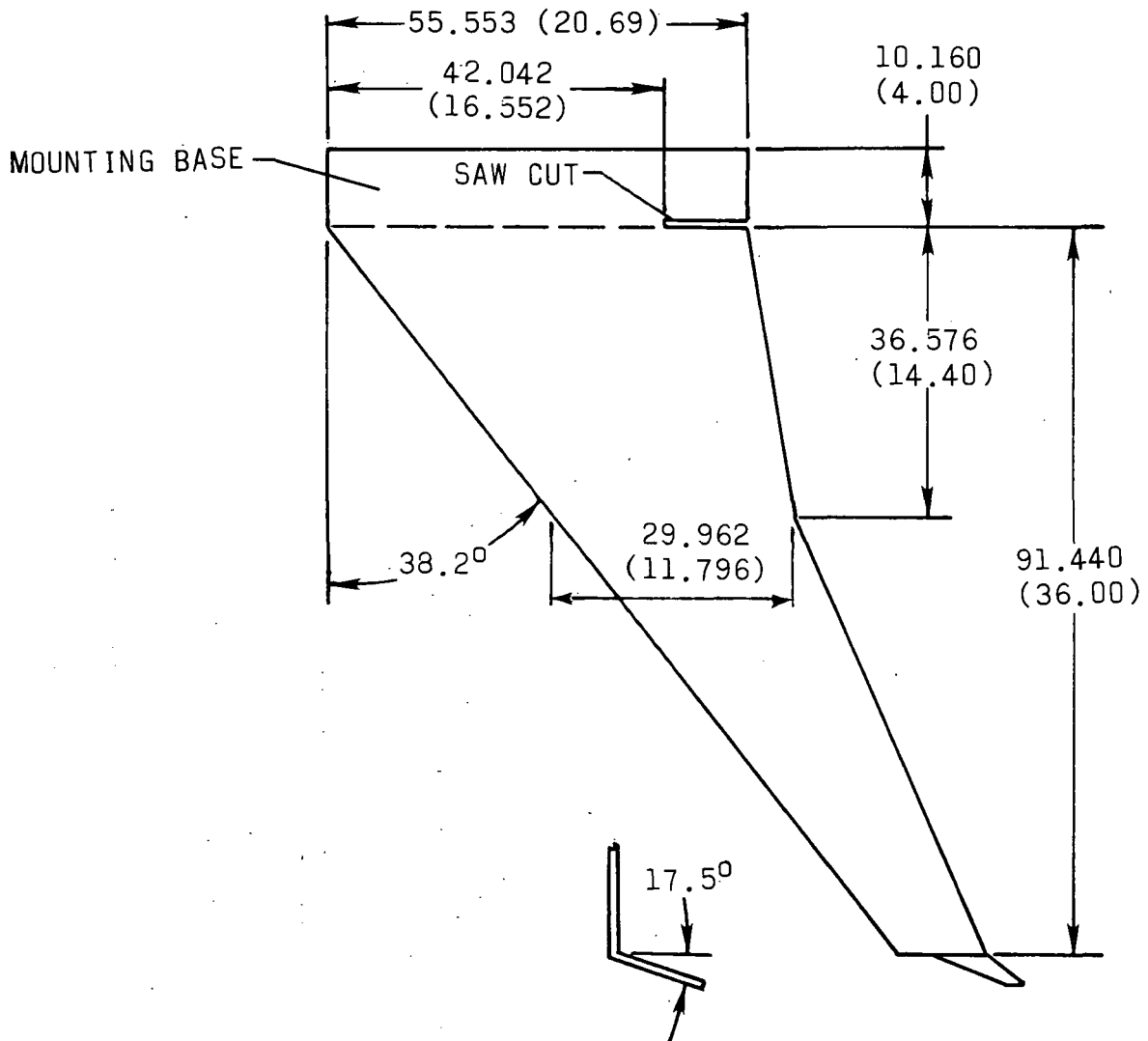
Model	Mode 1		Mode 2		Mode 3		Mode 4		Mode 5		Mode 6		Mode 7	
	$f_{e'}$ Hz	$f_{c'}$ Hz	$f_{e'}$ Hz	$f_{c'}$ Hz	$f_{e'}$ Hz	$f_{c'}$ Hz	$f_{e'}$ Hz	$f_{c'}$ Hz	$f_{e'}$ Hz	$f_{c'}$ Hz	$f_{e'}$ Hz	$f_{c'}$ Hz	$f_{e'}$ Hz	$f_{c'}$ Hz
Basic wing . . . . .	5.8	5.9	26.4	26.8	51.4	52.9	66.9	69.8	114.9	114.9	(a)	(a)	(a)	(a)
Light winglet . . . . .	5.7	5.8	25.8	26.2	51.1	50.7	(a)	53.8	68.3	68.3	(a)	114.5	(a)	130.6
Heavy winglet . . . . .	5.4	5.5	24.0	24.0	50.5	51.5	58.7	60.4	107.0	107.0	(a)	(a)	(a)	(a)

<sup>a</sup>Not determined.



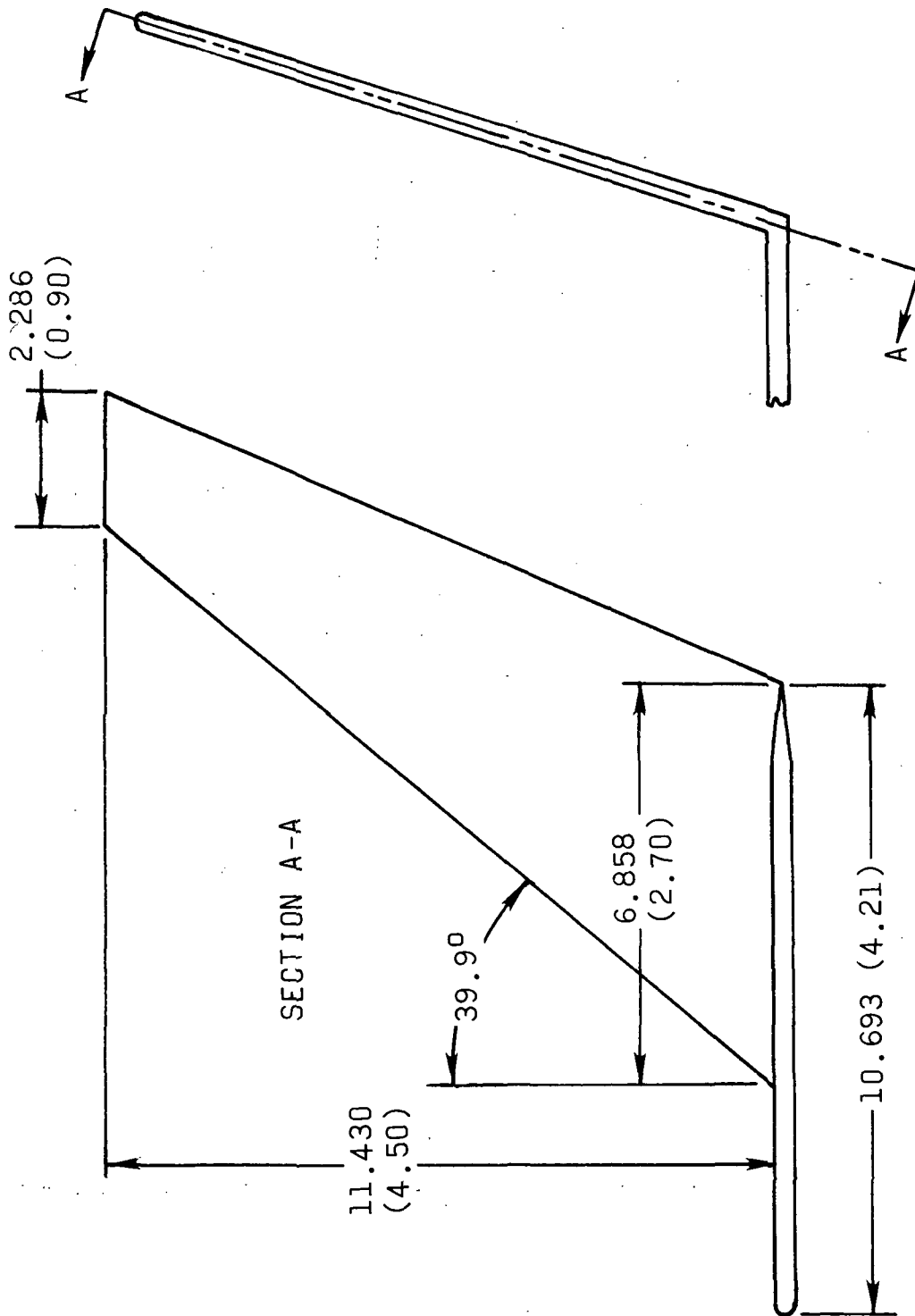
L-74-5170

Figure 1.- Photograph of heavy-winglet model mounted in wind tunnel.



(a) General layout and wing details.

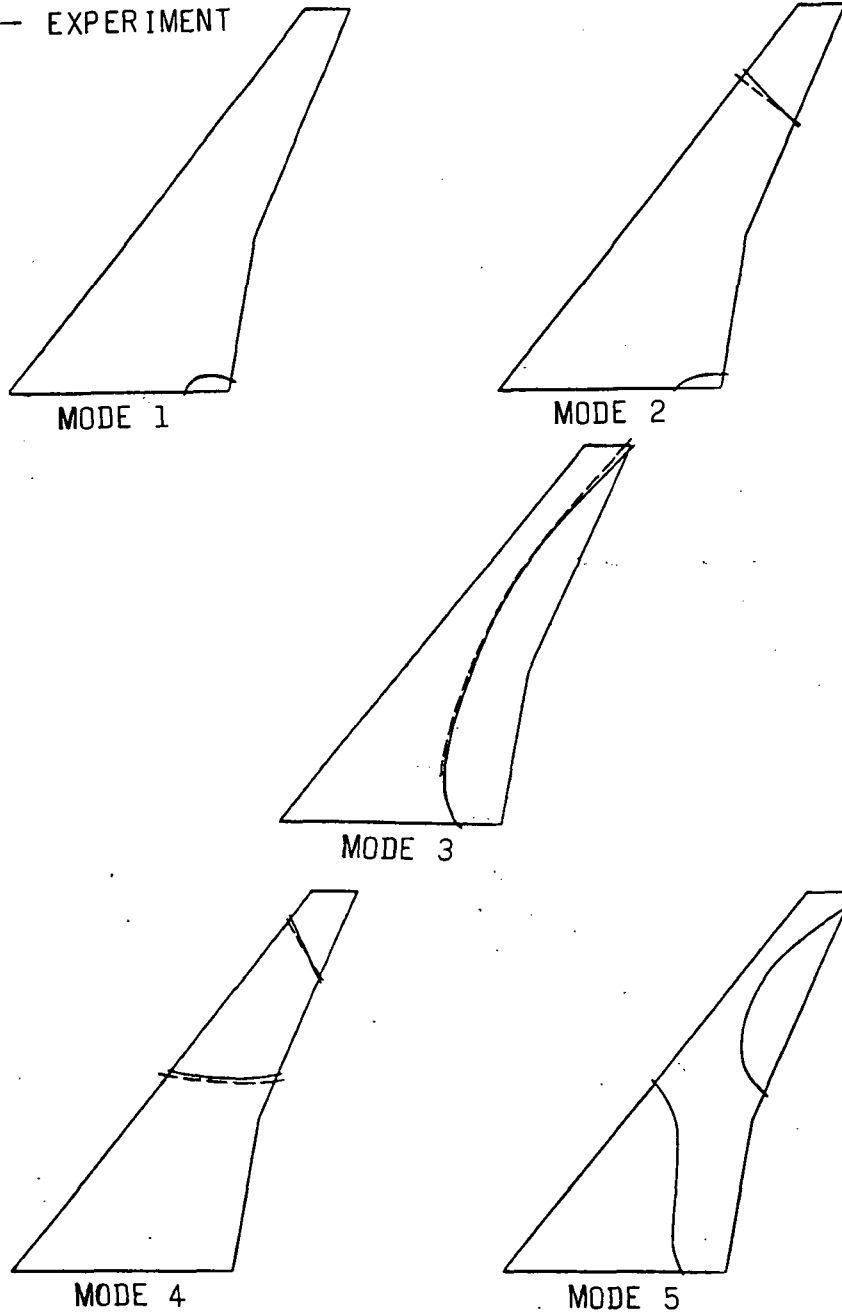
Figure 2.- Drawings of model configuration. Dimensions are in centimeters (inches).



(b) Winglet details.

Figure 2.- Concluded.

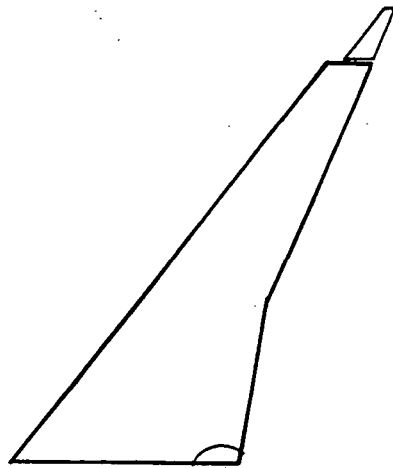
— CALCULATED  
- - EXPERIMENT



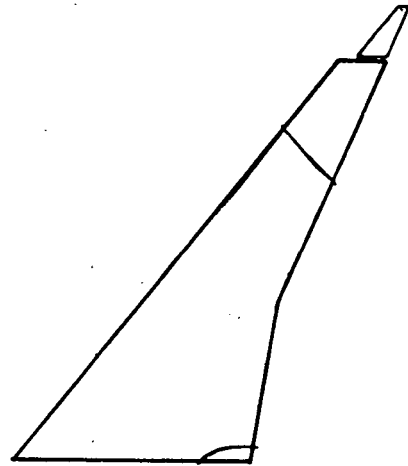
(a) Basic-wing model.

Figure 3.- Calculated and measured node lines.

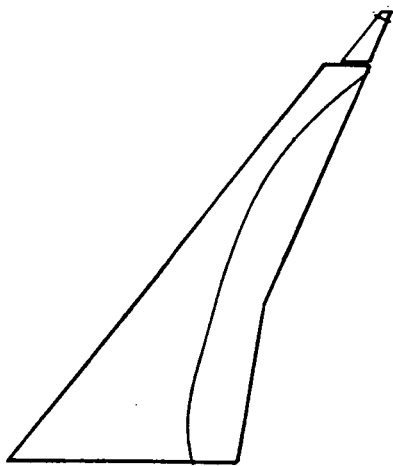
———— CALCULATED



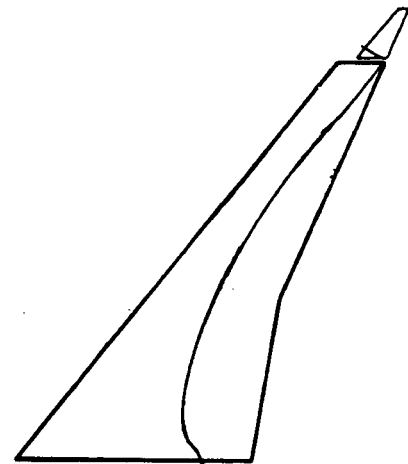
MODE 1



MODE 2



MODE 3

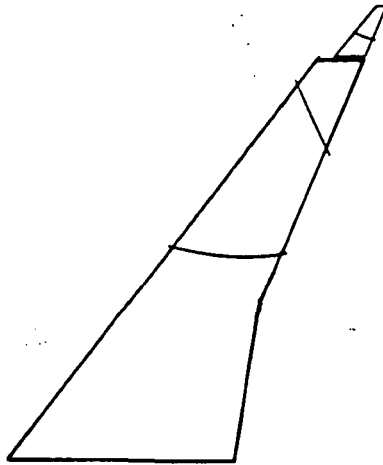


MODE 4

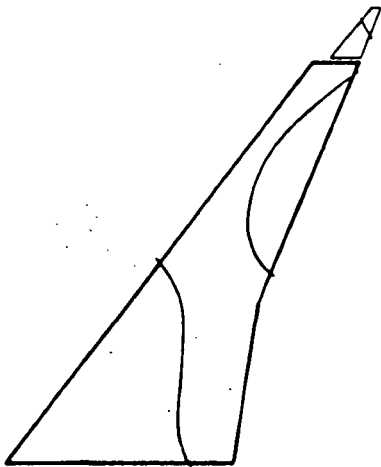
(b) Light-winglet model.

Figure 3.- Continued.

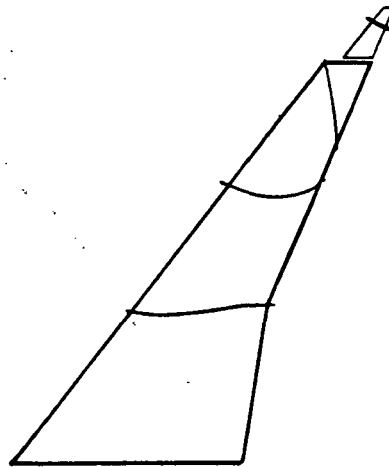




MODE 5



MODE 6

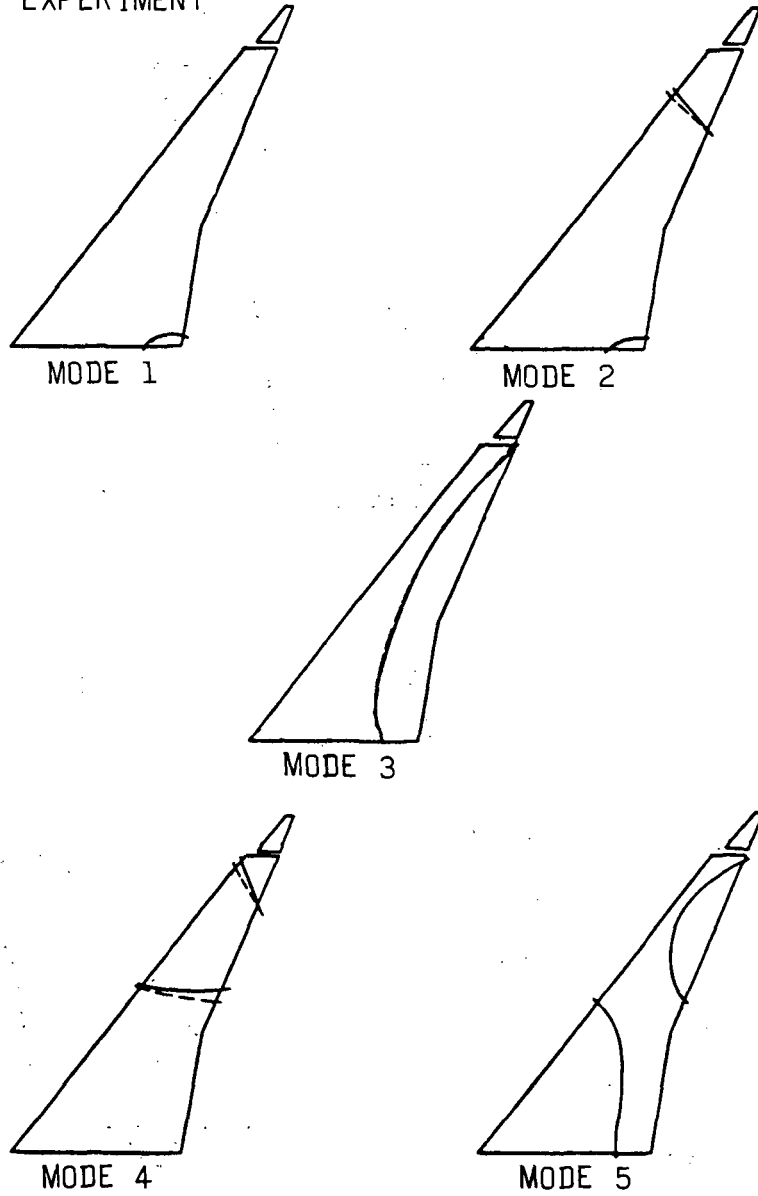


MODE 7

(b) Light-winglet model. Concluded.

Figure 3.- Continued.

———— CALCULATED  
- - - - EXPERIMENT



(c) Heavy-winglet model.

Figure 3.- Concluded.

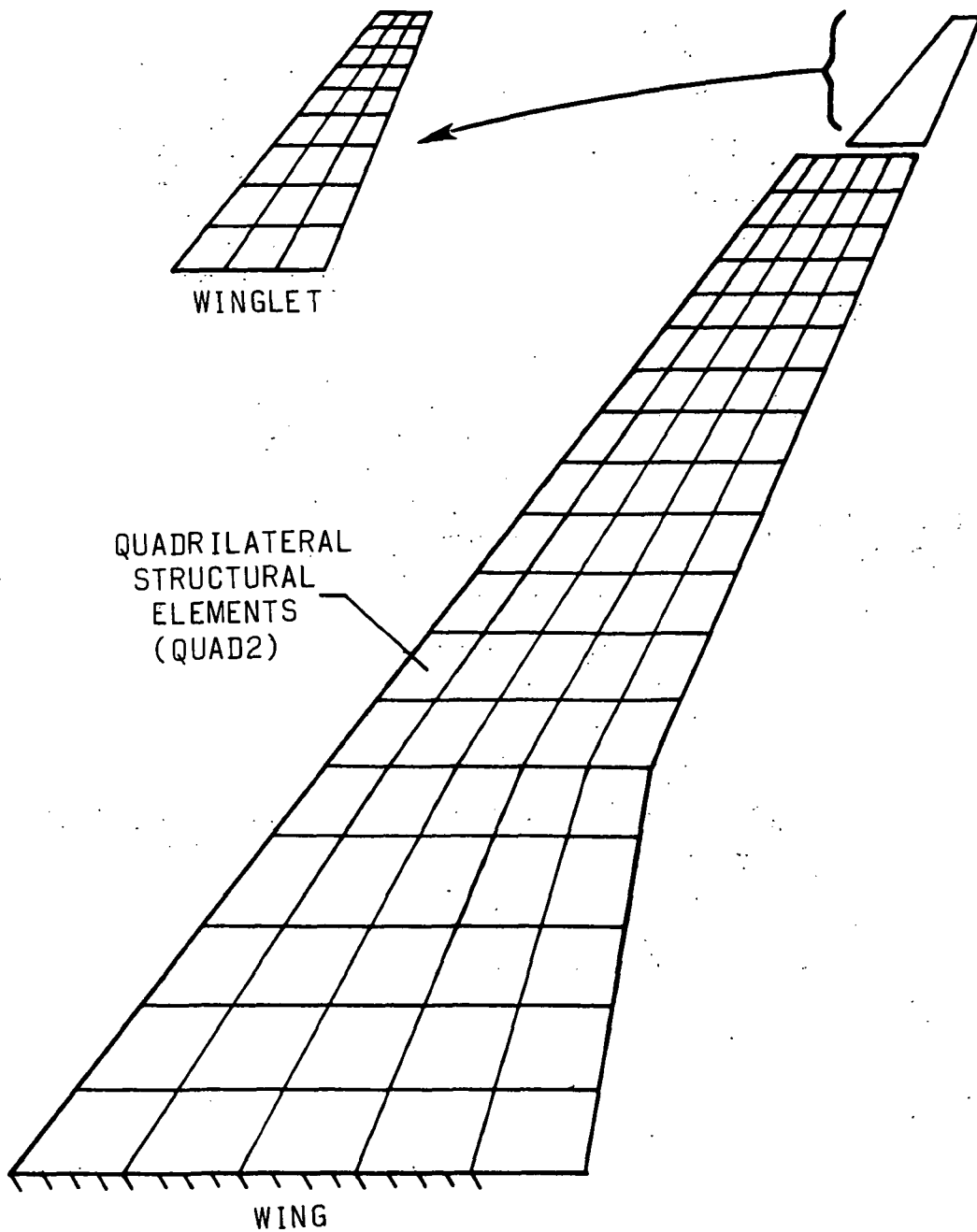


Figure 4.- NASTRAN<sup>®</sup> structural model.

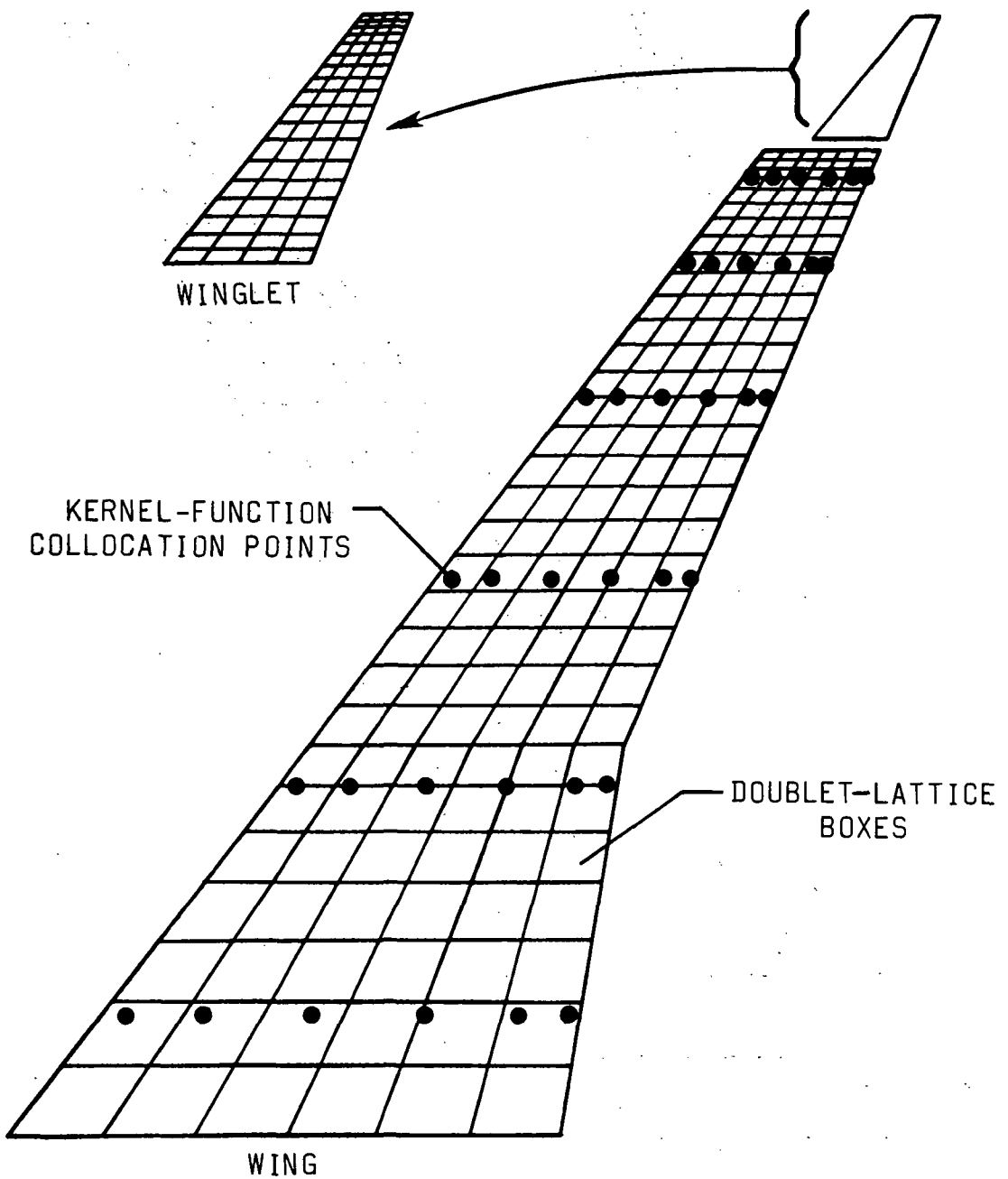
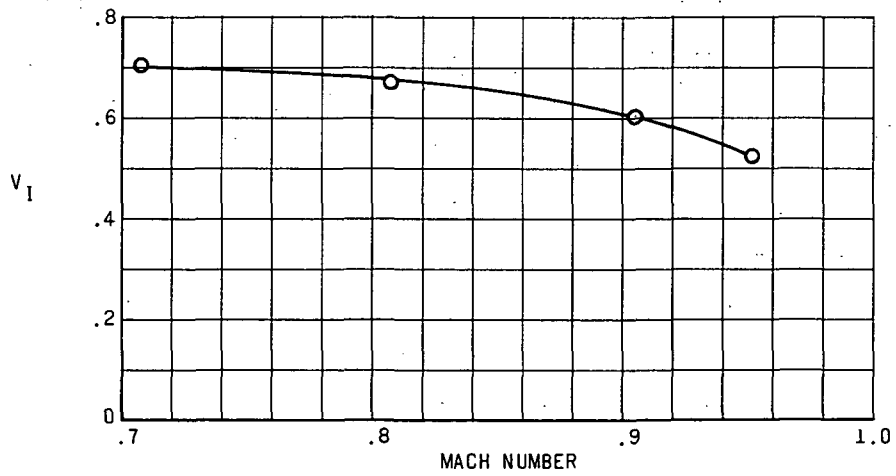
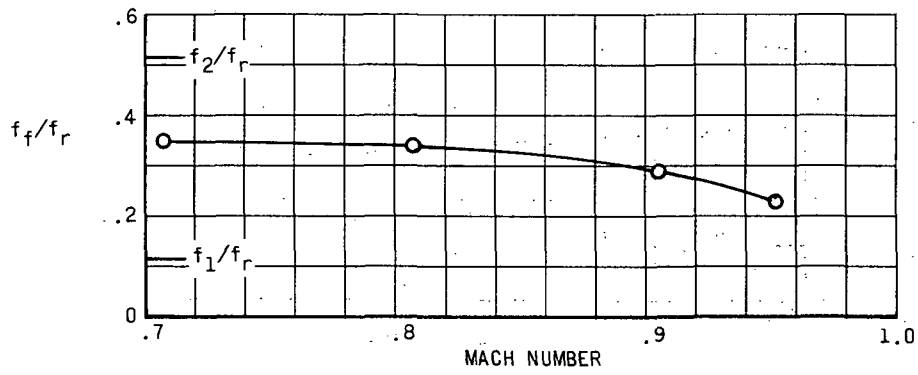
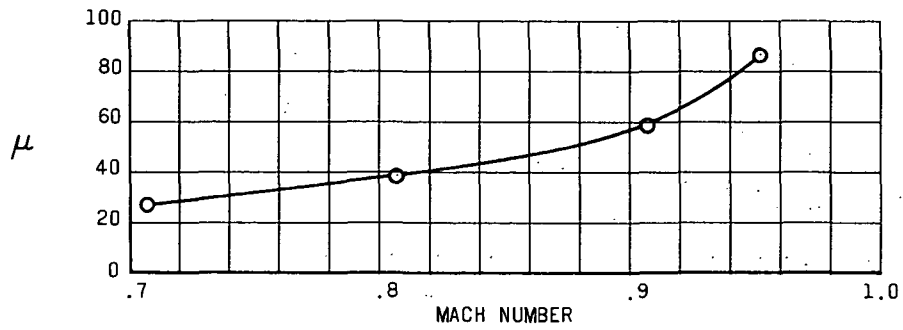
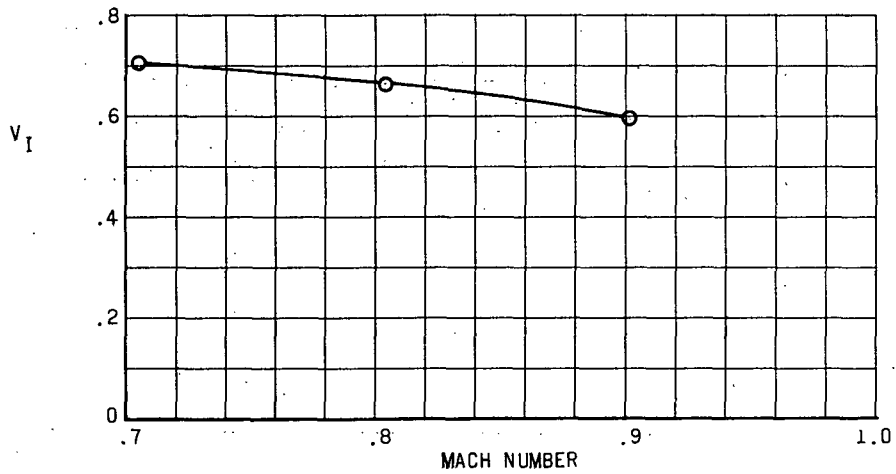
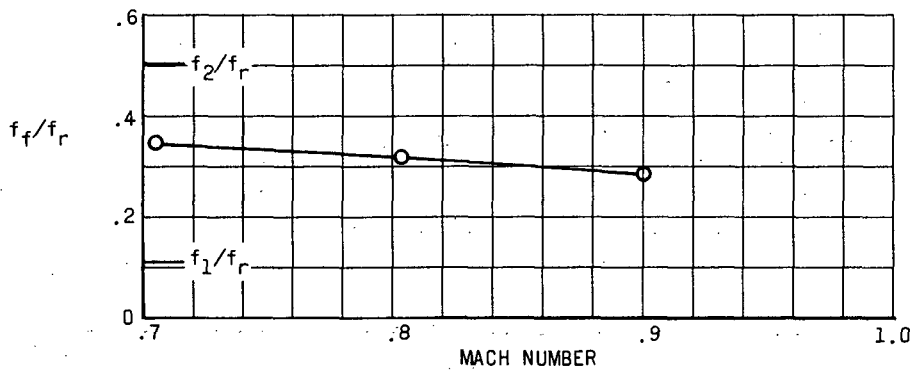
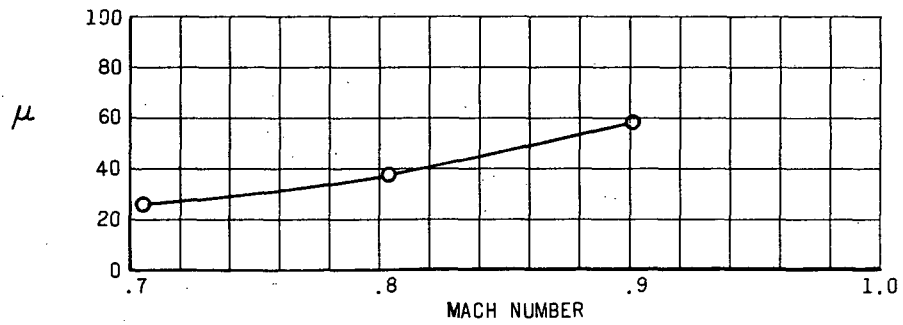


Figure 5.- Aerodynamic model.



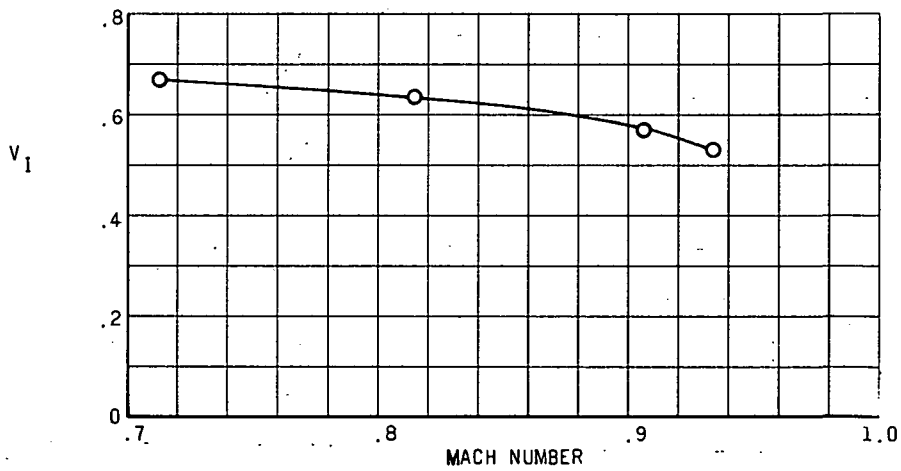
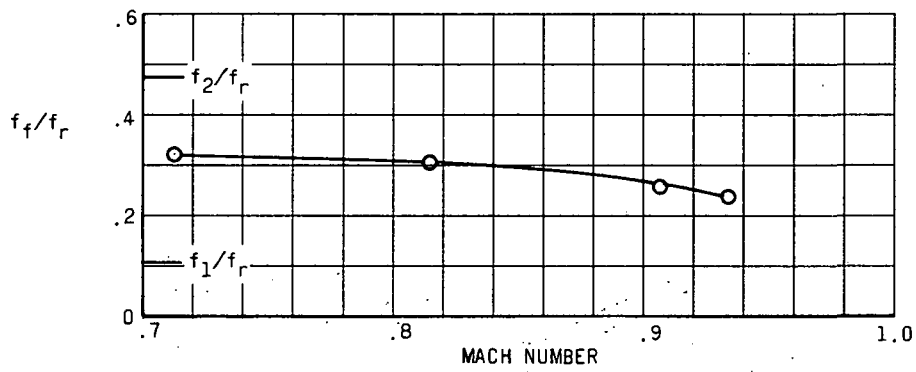
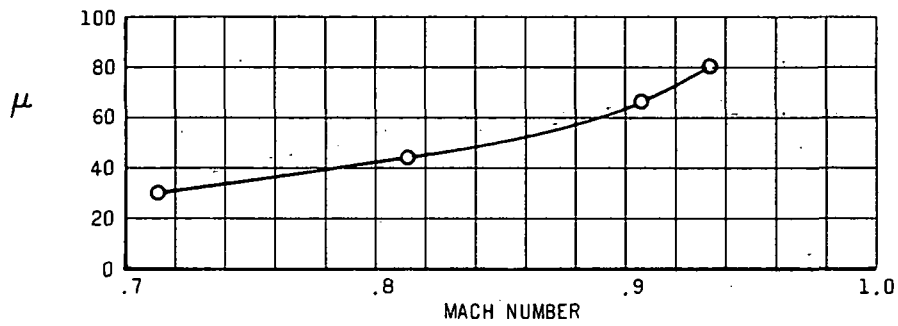
(a) Basic-wing model.

Figure 6.- Experimental flutter results.



(b) Light-winglet model.

Figure 6.- Continued.



(c) Heavy-winglet model.

Figure 6.- Concluded.

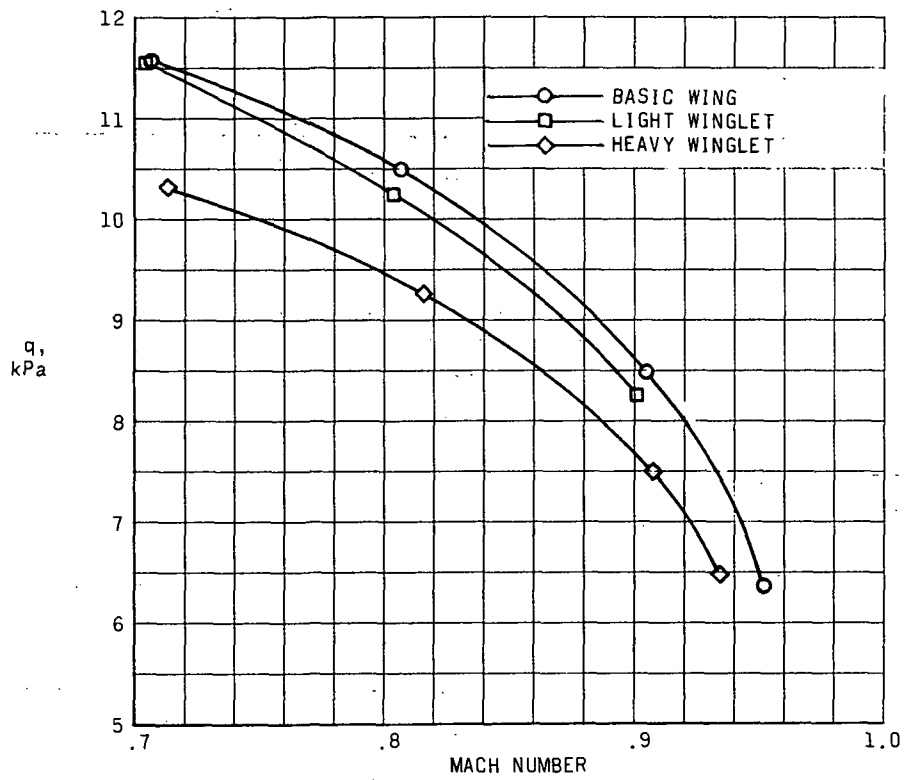
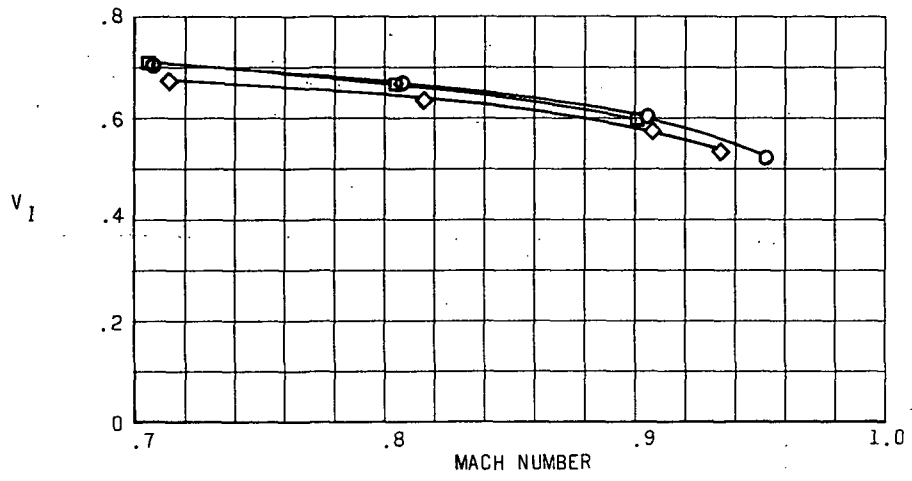


Figure 7.- Comparison of experimental results for the three models.



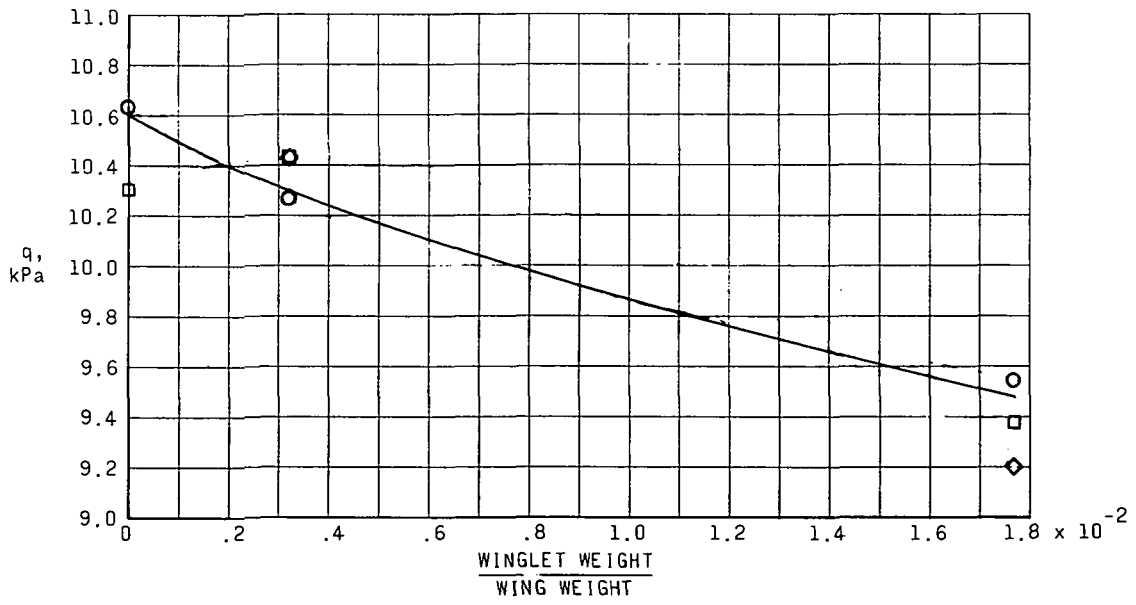
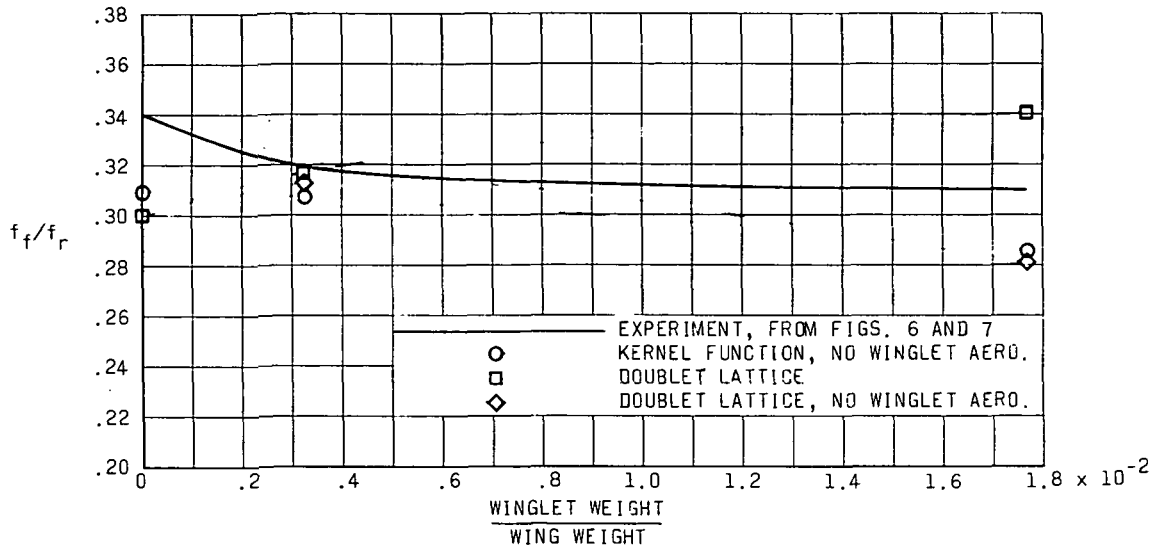


Figure 8.- Comparison of calculated and experimental flutter results.



POSTMASTER: If Undeliverable (Section 158  
Postal Manual) Do Not Return

*"The aeronautical and space activities of the United States shall be conducted so as to contribute . . . to the expansion of human knowledge of phenomena in the atmosphere and space. The Administration shall provide for the widest practicable and appropriate dissemination of information concerning its activities and the results thereof."*

—NATIONAL AERONAUTICS AND SPACE ACT OF 1958

## NASA SCIENTIFIC AND TECHNICAL PUBLICATIONS

**TECHNICAL REPORTS:** Scientific and technical information considered important, complete, and a lasting contribution to existing knowledge.

**TECHNICAL NOTES:** Information less broad in scope but nevertheless of importance as a contribution to existing knowledge.

**TECHNICAL MEMORANDUMS:** Information receiving limited distribution because of preliminary data, security classification, or other reasons. Also includes conference proceedings with either limited or unlimited distribution.

**CONTRACTOR REPORTS:** Scientific and technical information generated under a NASA contract or grant and considered an important contribution to existing knowledge.

**TECHNICAL TRANSLATIONS:** Information published in a foreign language considered to merit NASA distribution in English.

**SPECIAL PUBLICATIONS:** Information derived from or of value to NASA activities. Publications include final reports of major projects, monographs, data compilations, handbooks, sourcebooks, and special bibliographies.

**TECHNOLOGY UTILIZATION PUBLICATIONS:** Information on technology used by NASA that may be of particular interest in commercial and other non-aerospace applications. Publications include Tech Briefs, Technology Utilization Reports and Technology Surveys.

Details on the availability of these publications may be obtained from:

**SCIENTIFIC AND TECHNICAL INFORMATION OFFICE**

**NATIONAL AERONAUTICS AND SPACE ADMINISTRATION**

**Washington, D.C. 20546**